Polymers **2015**, *7*, 1279-1298; doi:10.3390/polym7071279

OPEN ACCESS

polymers

ISSN 2073-4360

www.mdpi.com/journal/polymers

Review

Turbulent Drag Reduction with Polymers in Rotating Disk Flow

Cheng Hai Hong [1], Chun Hag Jang [2,*] and Hyoung Jin Choi [1,*]

[1] Department of Polymer Science and Engineering, Inha University, Incheon 402-751, Korea; E-Mail: chenghaih@inha.ac.kr

[2] Department of Chemistry, Cheongju University, Cheongju, Chungbuk 363-764, Korea

* Authors to whom correspondence should be addressed; E-Mails: c1bs4a@hanmail.net (C.H.J.); hjchoi@inha.ac.kr (H.J.C.); Tel.: +82-32-860-7486; Fax: +82-32-865-5178.

Academic Editor: Alexander Böker

Received: 2 April 2015 / Accepted: 2 July 2015 / Published: 13 July 2015

Abstract: The frictional drag in turbulent flow can be drastically reduced by the addition of minute amounts of suitable linear flexible high-molecular-weight polymers, and the various physical characteristics of the polymers used are known to be closely related to the drag reduction efficiency. This feature article briefly reviews polymer additives and factors in the system affecting turbulent drag reduction in external flow, more specifically in a rotating disk flow.

Keywords: drag reduction; polymer; turbulent; coil–globule; rotating disk

1. Introduction

Turbulent flow is often described using the picturesque definition of "eddies within eddies within eddies" [1]. It is ubiquitous in nature and in engineering applications associated with the most flow. The dissipated energy losses due to turbulent friction are quite large, and this provides enough motivation to find ways to reduce it. As compared to passive drag reduction efforts, which make use of riblets, as well as wavy and micro-bubbles, the active drag reduction (DR) in a turbulent flow has attracted significant interest by the addition of minute amounts of suitable polymers or surfactants [2–4]. Very dilute polymer solutions undergoing flow in a pipe generally require a lower pressure drop to maintain the same volumetric flow rate. In other words, a higher flow rate will be obtained for the same pressure drop for a turbulent polymeric solution compared to the flow with just a solvent medium. Because this DR

phenomenon was first observed by Toms for tiny additions of polymethylmethacrylate to the turbulent pipe flow of monochlorobenzene, it is often referred to as the "Toms effect" [5]. Since then, the study of turbulent DR has been the subject of intensive theoretical and experimental studies owing to its application to engineering and to its scientific interest mainly in terms of pipe flow. However, the phenomenon of DR in external flow and two-dimensional flow has been also investigated.

In pipe flows, the percentage drag reduction effectiveness, DR(%), has been reported to be the ratio of either the friction factor (f) or the pressure gradient (Δp) of the DR solution to that of the solvent medium either at a constant flow rate or at constant Reynolds number, respectively, in the same pipe [6]. Concurrently, the DR efficiency can be defined by

$$DR(\%) = \left(\frac{f_s - f_a}{fs}\right) \times 100 = \left(\frac{\Delta P_s - \Delta P_a}{\Delta P_s}\right) \times 100 \quad (1)$$

where f_s and f_a, are the friction factors, Δp_s and Δp_a are the pressure gradients for the pure solvent medium and solution with an additive, respectively. Among various types of additives such as solid particles, polymers [7,8], and surfactants [9–11], linear flexible polymers—those are the ones without branches—are known to be the most effective DR agents. Even carbon nanotubes by themselves do not provide DR in a turbulent flow, it was recently reported that carbon nanotubes can enhance the drag-reducing characteristics of polymer additives [12]. The polymer or surfactant additives were found to strongly influence the turbulence behavior, which has broadened the range of possibilities for turbulence manipulation in engineering applications [13]. Some examples of engineering applications of polymer or surfactant additives include crude oil pipeline transportation [14], slurry transport [15], and biomedical applications [16].

This feature review article focuses on the DR of polymer additives in turbulent flow, not only because of the DR phenomena associated with turbulence itself but also because of the nonlinear interaction between the flow and the polymers, which has been reported to be of fundamental importance in terms of various experimental parameters. Nonetheless, we focus here on rotating disk flow, which represents external flow such as flow around submerged objects and Couette flow. It is of note that one studies typical friction drag for internal flow, whereas for external flow, one can study the total drag of friction plus form drag, in which the turbulent DR is known to be related mainly to friction drag.

2. Mechanism of DR

Although the mechanism of turbulent DR is not completely understood, it is believed that more than one kind of DR mechanism exists, and experimental findings suggest that the region near the wall plays a critical role in DR occurring in turbulent pipe flow of very dilute solutions of macromolecules [17]. During flow, the polymer molecules affect the region near the wall most strongly. However, in the flow near the wall, shear thinning does not always occur because the shear viscosity difference between the drag-reducing solution and the solvent is sometimes very small.

On the other hand, considering the viscoelastic behavior of drag-reducing polymer solutions near a wall, measurements of the normal stress difference or the thrust from a jet of the polymeric fluid have indicated viscoelastic effects as a source of the DR [18]. To be replaced by other elements, the elastic stress of an element moving along the wall must first be relaxed in order for the viscous deformation

required for its replacement to occur. This introduces a delay in the replacement process in comparison to the behavior of a Newtonian fluid. As the instantaneous shear stress at the wall decreases with increasing contact time with the wall, the average shear stress at the wall decreases. Furthermore, Lumley [19] showed that turbulence is not sensitive to shear-induced changes in viscosity, which is in turn dominated by inertial forces, thus explaining the mechanism of DR as a molecular extension. The linear polymeric molecules could be greatly extended in the shear direction, thus providing a stiffening effect, which absorbs energy from the turbulent eddies, resulting in the turbulent DR phenomenon.

By relating viscoelasticity with energy dissipation further, Astarita [20] suggested that turbulence in viscoelastic liquids is less dissipative than in Newtonian fluids, while Gadd [21] proposed that DR occurred not due to reduced turbulence dissipation but rather to a decrease in turbulence production. Walsh [22] proposed a comprehensive theory of DR such that large-scale disturbances, which produce Reynolds stresses at some distance downstream, were previously small disturbances at the edge of the viscous sublayer at some distance upstream. These small-scale disturbances tend to pump energy into the polymer molecules. The polymer molecules then help by altering the energy balance of the turbulent fluctuations close to the wall, thus allowing viscous dissipation to destroy the disturbances. By decreasing the number of disturbances moving out from the viscous sublayer, the addition of the polymer molecules ultimately changes the structure in the outer part of the boundary layer, resulting in lower Reynolds stresses and hence reducing drag. Nonetheless, Walsh's theory does not predict turbulence dampening in free flow, because it is based upon the assumption that the phenomenon is essentially due to the existence of wall–boundary–layer flow.

An alternative mechanism is the development of resistance to vortex stretching owing to the presence of the additives. Based on the concept of vortex stretching, Gadd [23] suggested that vortex stretching occurs along the wall and that the elongation of the molecules causes large tensile forces along the streamline, which inhibit vortex stretching to give reduced mixing and more rapid decay of eddies. Larger polymers, with longer relaxation times, would probably affect the large eddies with less intense stretching rates and cause them to decay more rapidly. Further support of vortex-stretching inhibition on the basis of increased elongational viscosity has been proposed as an effective factor on turbulent eddy generation and growth [24]. Gordon and Balakrishnan [25] also explained the DR phenomenon as resistance to vortex stretching caused by filament formation in drag-reducing polymer solutions.

On the other hand, by adopting a simple model to study both turbulence and the dissolved polymer molecules, Armstrong and Jhon [26] constructed a self-consistent method from the relationship between molecular dissipation and the friction factor. They also examined the importance of elastic properties to describe the DR mechanism. For polymer molecules, they used a variant of the dumbbell model. The dumbbell model, initially proposed by Fraenkel [27], represents a polymer molecule dissolved in a solvent by considering the polymer molecule as two spherical identical beads connected by a central spring immersed in an otherwise Newtonian fluid. Turbulence was also modeled by keeping a kinetic energy budget on the overall flow. They found that a polymer molecule grows by a factor of 10 or more from its equilibrium conformation.

Concurrently, mechanical chain degradation of polymer additives in turbulent flow has also been regarded as crucial, especially for their engineering applications. Among various efforts to explain the DR phenomena as a result of mechanical degradation in flow, Brostow [28] developed a statistical–mechanical model of polymer chain conformation and showed that the obtained solvation

numbers were well correlated with their theory, which explains DR in dilute polymer solutions in terms of the solvation of macromolecular chains and the formation of relatively stable, energy-sinking domains [29]. On the other hand, an elastic theory of DR was introduced to discuss the properties of homogeneous, isotropic, three-dimensional turbulence in the presence of polymer additives with no wall effect [30]. The central idea of this "cascade theory", which is limited to linear flexible chains in a good solvent, is that small-scale polymer effects are not described by the viscosity but by the elastic modulus. Recently, the effect of viscoelasticity on the turbulent kinetic energy cascade was also reported [31].

In general, these long-chain polymers will be broken by the turbulence and DR will be degraded soon after the polymers are added. It was found that this mechanical molecular degradation and DR efficiencies are correlated [32]. It has been reported that the fibers, being rigid, degrade less than linear flexible polymers, although it is true that the DR level is lower [33,34]. After finding that the single exponential decay model is not universally suitable for all polymeric drag reducers [32], Choi *et al.* [35] investigated the applicability of a simple first-order degradation model and the Brostow Equation.

The simple first-order degradation model was used to fit the DR efficiency as follows:

$$\begin{aligned} \%\mathrm{DR}(t) &= w(L)N_{\mathrm{L}}(t) + w(L/2)N_{\mathrm{L}/2}(t) + c \\ &= w_1 \mathrm{e}^{-at} + 2w_2(1 - \mathrm{e}^{-at}) + c \end{aligned} \tag{2}$$

where $w(L)$ is the drag-reducing power dependence, $N_{\mathrm{L}}(t)$ and $N_{\mathrm{L}/2}(t)$ are the number of polymers with lengths L and $L/2$ at time t, respectively, and w_1, w_2, and c are the fitting parameters. The rate constant a, with units of reciprocal time (1/s), contains information on the dynamics of mechanical degradation of the polymer chain.

As an another model, the Brostow equation describing the deteriorating DR efficiency has been also suggested [36], as in the following form:

$$\mathrm{DR}(t)/\mathrm{DR}(0) = 1/[1 + W(1 - \mathrm{e}^{-ht})] \tag{3}$$

where the parameter W is related to the shear stability and the parameter h is related to the degradation rate, and is a constant for a given Reynolds number and polymer/solvent pair while depending on polymer concentrations. Therefore, at a given Reynolds number and polymer concentration, h can be estimated. A large h value indicates rapid degradation, whereas a larger W value implies low shear stability. In addition, more terms for h were suggested, which is now a function of the polymer concentration.

Pereira and Soares [37] also proposed a model to compute the relative drag reduction as a function of Reynolds number, polymer concentration, molecular weight, and temperature, by estimating the developing time as a function of the concentration, molecular weight, Reynolds number, and temperature using a commercial rotational rheometer with axial symmetric double gap and Taylor–Couette geometries. Their model clearly shows that the developing time is more sensitive to temperature variations, while being equally affected by variations in concentration and in molecular weight. Nonetheless they needed the development time because the turbulent structures from this rotational rheometer require some time to develop and achieve a steady state, while the rotating disk flow in this study does not require the development time due to instantaneous mixing.

3. Rotating Disk Flow

Up to now, to analyze turbulent DR, most research groups have adopted the pipe flow [38–41], which produces a pressure-driven flow in an enclosed channel as an internal flow. In contrast, a high-precision rotating disk apparatus system [42] has been used for measuring DR in an external flow as a function of time. It has also been recently discovered that rotating disks can reduce turbulent drag by themselves if placed underneath a fully developed turbulent flow [43–45]. The percentage DR is calculated as:

$$DR\% = (\frac{T_S - T_P}{T_S}) \times 100 \quad (4)$$

where T_s is the measured torque of the solvent alone and T_p is the measured torque of the polymer solution at a constant angular velocity of the disk at a fixed rotation speed. The pipe flow and rotating disk apparatus (RDA) system flow are shown schematically in Figure 1.

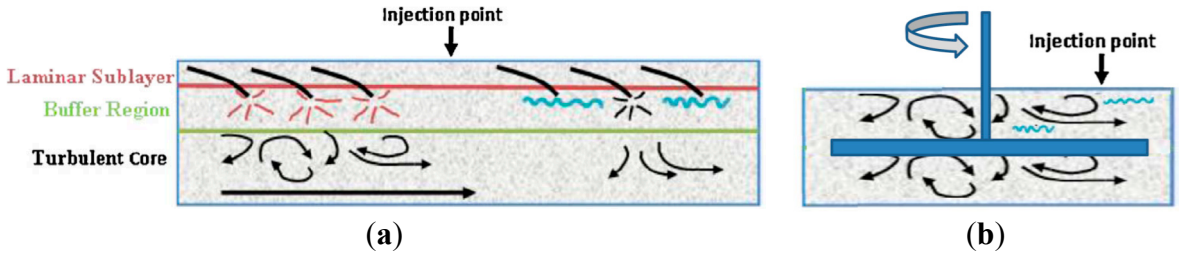

Figure 1. Schematic diagram for the methods of added polymer to solution with (**a**) pipeline turbulent flow (Reprinted from [3]) and (**b**) rotating disk apparatus (RDA) turbulent flow.

The rotating disk apparatus system, interfaced with a computer control unit, combines high-speed data sampling with controlled disk rotational speed in order to accurately measure fluid friction from laminar to turbulent flow [42]. The gravity-driven method [46], two counter-rotating bladed disks systems [47], and a Taylor–Couette device [48] have also been used for measuring DR. In addition, direct numerical simulations and statistical analysis techniques are used to study the drag-reducing effect of polymer additives on turbulent channel flow in minimal domains [49,50]. Furthermore, one of the big advantages of this rotating disk flow is that the mixing time of the polymer with the flow can be estimated as the turnover time of the largest eddies which is always less than the 0.2 s injection time. Since all the data reported using this geometry are sampled in the time scale of a few seconds, the mixing of polymers with the flow in these experiments can be considered as instantaneous mainly due to a very high rotation speed of the disk [35].

While most of all the DR studies have been made in three-dimensional (3-D) flow, two-dimensional (2-D) flows different to the 3-D flow were adopted for DR studies [51–53], mainly using soap film flows, as shown in Figure 2 [52],

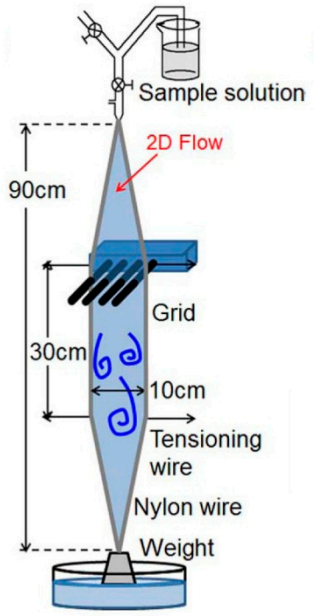

Figure 2. Schematic diagram of experimental set-up of flowing soap films (Reprinted from [52]).

4. Polymer Concentration Effect

In general, the DR efficiency in turbulent flow increases as the added polymer concentration increases until a certain polymer concentration is reached at a fixed Reynolds number. As shown in Figures 3 and 4, beyond the certain polymer concentration, a further increase in concentration leads to a leveling-off or a decrease in the DR. Above this concentration, the DR efficiency tends to decrease [54,55]. This behavior is considered to be due to the combination of two factors: the initial increase in DR is presumably due to the increasing number of polymer molecules present, which causes the decay of turbulent eddies, whereas the shear viscosity becomes increasingly significant at higher concentrations of polymer, and the Reynolds number decreases compared to that of the initial state. Furthermore, the overshoot of the DR at c = 50 ppm for Figure 4 was explained by the Brownian dynamics simulation results showing that partial disentanglement of entanglements that existed at rest takes place in flow [29,55,56]. Zhang *et al*. [55] considered that further addition of the DR agent does not change that DR efficiency since much of the solvent is already solvated by the DR agent chains. When more polymer is added, the solvated domains might even get smaller since there is now a competition of sorts of the polymeric chains for the solvent molecules. On the other hand, as shown in Figure 5, Ram *et al.* [57] also found that the DR efficiency of commercial guar gum, purified guar gum, and grafted guar gum increased as the polymer concentration increased.

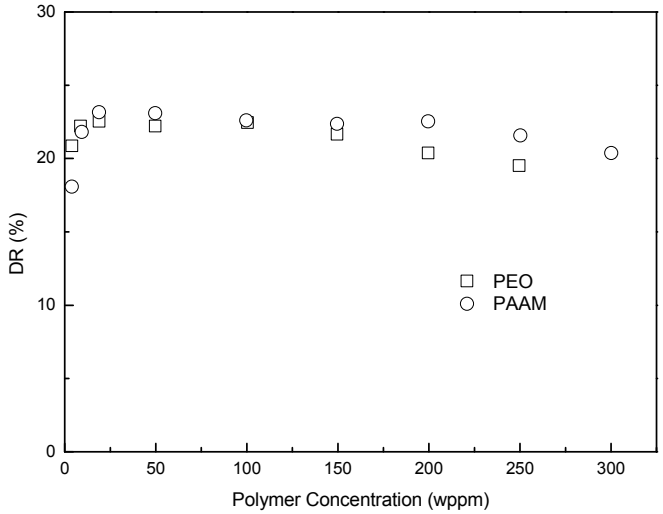

Figure 3. Drag reduction (DR) efficiency as faction of poly(ethylene oxide) (PEO), and polyacrylamide (PAAM) concentration (Reprinted from [54]).

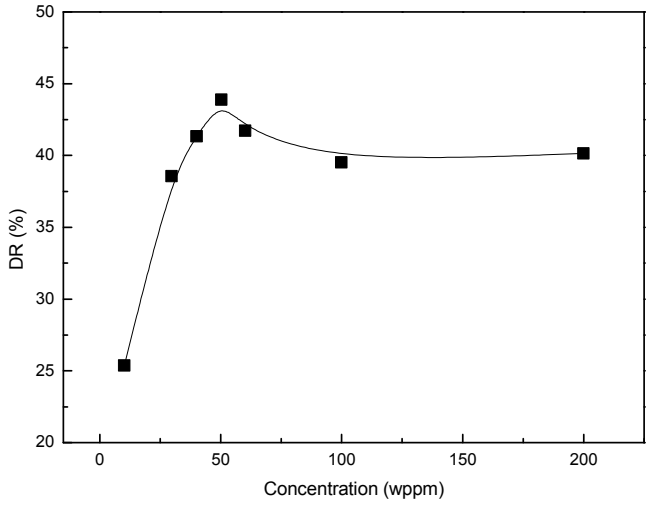

Figure 4. %DR *versus* concentration of poly(AM-*co*-AA) copolymer at 1980 rpm (Reprinted from [55]).

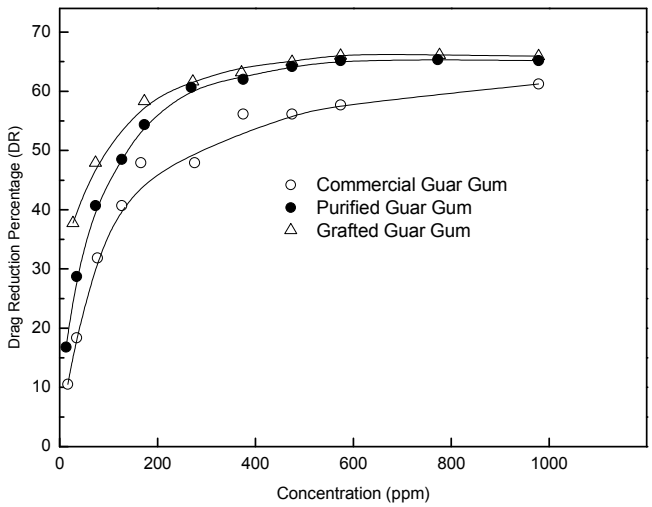

Figure 5. DR of commercial guar gum, purified guar gum, and grafted guar gum in a pipe flow (Reprinted from [57]).

Polymer concentration is also known to be quantitatively related to drag reduction effectiveness of randomly coiled polymer solutions such as water-soluble poly(ethylene oxide) (PEO), polyacrylamide (PAAM) and its copolymer [54,55,58], xanthan gum [59], amylopectin [60], DNA [61], guar gum [62], and so on (Figures 6–8). On the other hand, White *et al.* [63] observed that the concentration of the polymer is not uniform in the streaks and that the spatial distribution of the polymer is related to the turbulent structure.

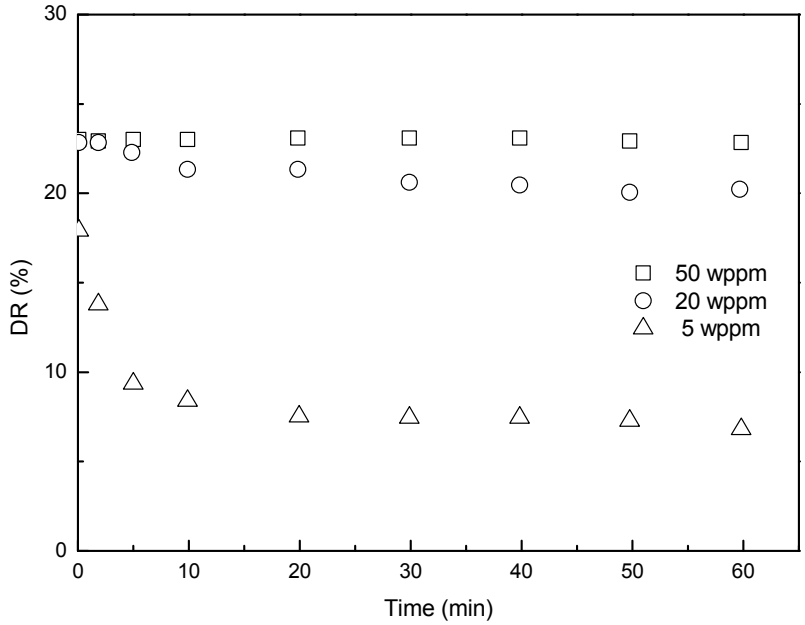

Figure 6. DR as a function of time at 2800 rpm for three different PAAM (Reprinted from [54]).

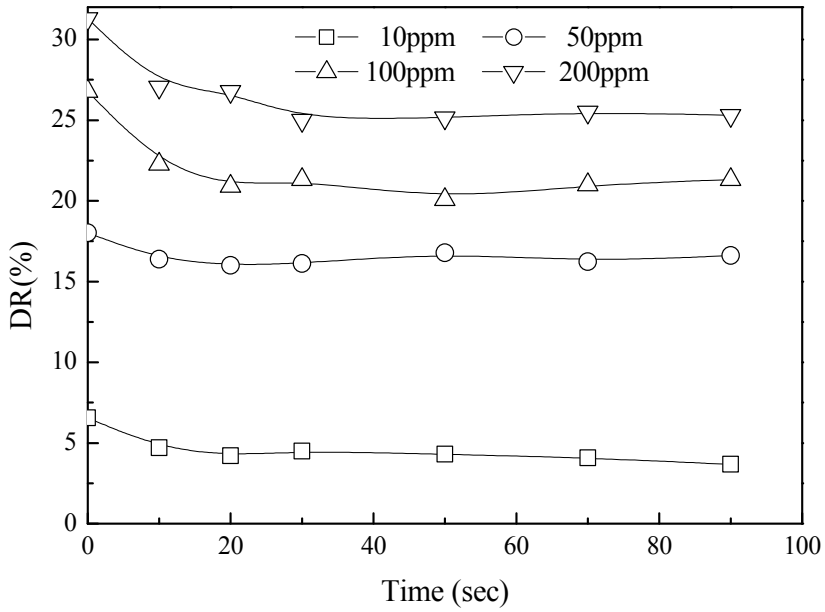

Figure 7. Drag reduction *versus* time with virgin guar gum and different concentrations (Reprinted from [62]).

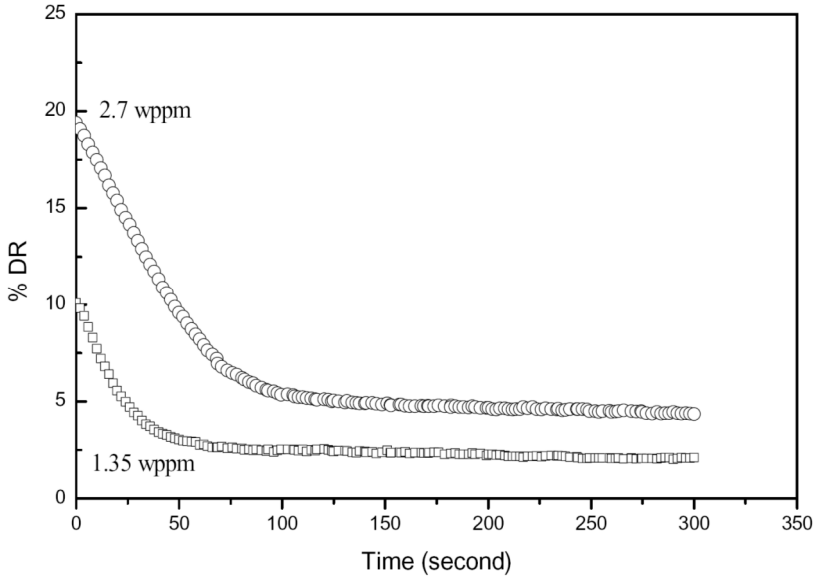

Figure 8. Drag reduction *versus* time with λ-DNA and different concentrations (Reprinted from [35]).

5. Polymer Chain Conformation Effect

Linear polymers without branches are regarded as more effective drag reducers than polymers with other nonlinear structures. PEO, one of the most flexible polymers, could be the most effective polymer drag reducer. The effectiveness of polymer chains in turbulent flow depends on the stretching of individual molecules by the stresses in the flow. However, in the case of amylopectin, the situation could be different. Although amylopectin did not show any noticeable DR effect grafted amylopectin at the same concentration exhibited much higher DR efficiencies [60].

The effect of molecular conformation on DR by changing the interactions between polymer molecules and solvent has also been examined. The drag-reducing ability of oil-soluble polyisobutylene was found to be better in a good solvent than in a poor solvent [64], indicating that DR in good solvents, which allow polymer molecules to expand more freely in the solution, is greater than in poor solvents, where the polymer molecule's hydrodynamic volume decreases and the polymer chain segments stay close to each other.

Furthermore, Sohn *et al*. [65] demonstrated that molecular conformation can also be altered by changing the salinity of an aqueous xanthan gum solution. They found that xanthan gum in salt aqueous medium produced more DR than in water solutions. The polymer molecules expanded in the former solution due to charge repulsion and coiled in water solutions in which charges are neutralized.

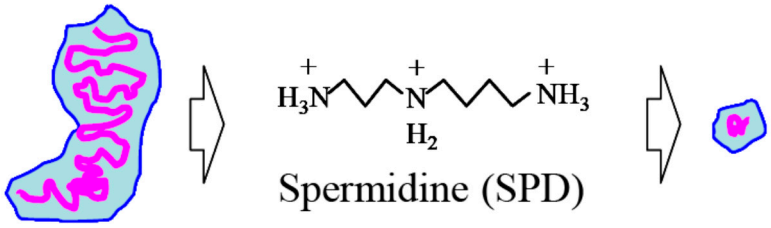

Figure 9. Coil-globule transition of DNA by SPD (Reprinted from [66]).

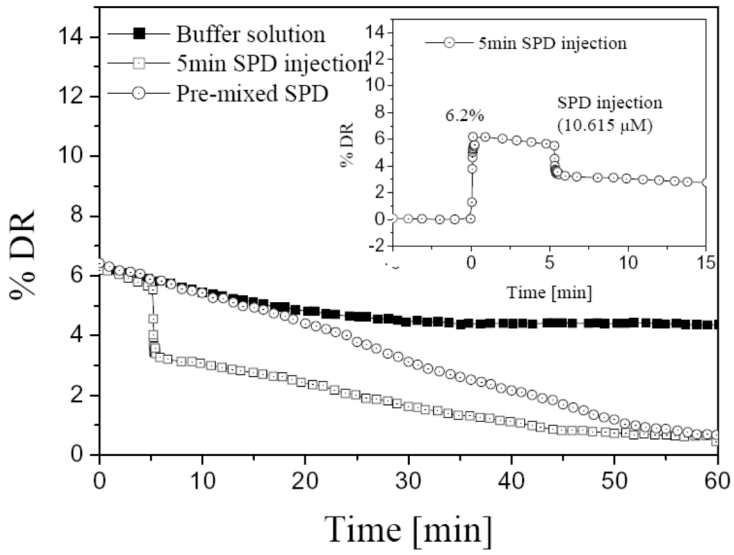

Figure 10. The percent drag reduction *versus* time for 1.35 wppm λ-DNA in buffer solution at 1157 rpm ($N_{Re} = 5.9 \times 10^5$) and 25 °C with and without spermidine (SPD). The inset shows the magnification of initial change of DR by SPD injection (Reprinted from [66]).

On the other hand, by applying the coil–globule transition concept of DNA to turbulent DR phenomena, the structural effect on the DR can be evidently and dramatically examined [66]. The addition of spermidine (SPD) into turbulent flow as a condensing agent of lambda-DNA showed a sudden decrease of drag-reducing efficiency (Figures 9 and 10). Lambda-DNA was reported to be a better drag reducer than linear polymers of PEO (Figure 11) and PAAM (Figure 12). Interestingly, in terms of its mechanical degradation, lambda-DNA is always being cut in half [35,61]. This means that the degradation mechanism for DNA is different from that of synthetic linear polymers. PAAM, however, showed much higher drag-reduction efficiency in the beginning, but it eventually diminished to zero within 5 min, as shown in Figure 9 in a rotating disk flow.

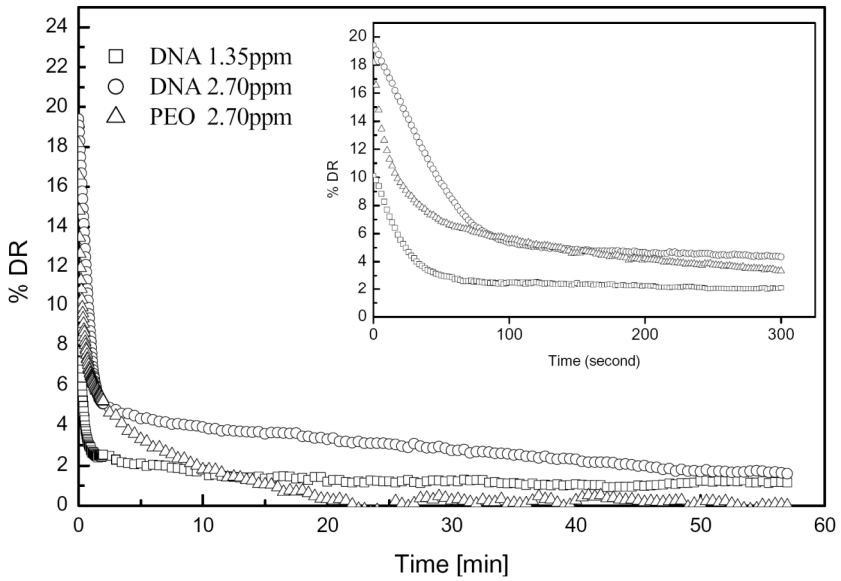

Figure 11. DR for 1.35 and 2.70 wppm λ-DNA in buffer solution compared with PEO (Mw = 5 × 10^6) at 1980 rpm. Inset shows the same data at early times (Reprinted from [35]).

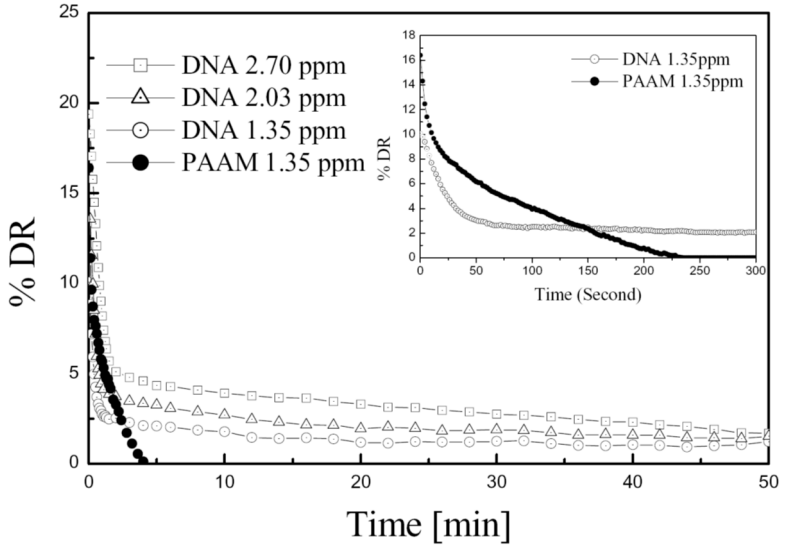

Figure 12. Comparison of λ-DNA percent drag reduction (1.35, 2.03, and 2.70 wppm) with PAAM (*M*w) 18 × 10^6 g/mol) on long-term scale (1 h) at 1980 rpm (N_{Re}) 1 × 10^6) and 25 °C. The inset represents the initial changes in the drag reducing efficiency for λ-DNA and PAAM at 1.35 wppm (Reprinted from [61]).

The DR efficiency of double-stranded and single-stranded chains from the same lambda-DNA was also examined [35]. In order to change the structure of DNA from a double-stranded to a single-stranded state in solution, experiments with distilled water were performed. Note that DNA can be denatured from a double-stranded natural state into two single-strand molecules. When the DNA is denatured, DNA molecules will be split into two single strands. Its behavior is similar to that of normal long flexible chain linear polymers, as found in the distilled water experiment with DNA shown in Figure 13. It also shows that the DR power of DNA in buffer solution is approximately twice that in distilled water before degradation. It is clear that double-stranded DNA is a better drag reducer than single-stranded DNA in the sense that not only does double-stranded DNA give a higher %DR efficiency for the same concentration, it also possesses greater resistance to degradation.

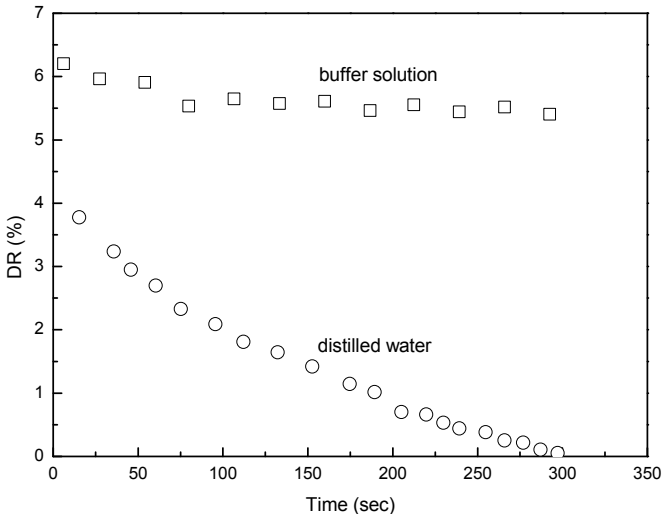

Figure 13. Difference between measured %DR of 1.35 wppm λ-DNA at *Re* = 7 × 10^5 in buffer solution and distilled water (Reprinted from [35]).

6. Molecular Weight and Polydispersity Effect

At the same polymer concentrations, long-chain drag-reducing macromolecules are known to be more effective. However, the effect becomes complicated due to the polydispersity of the polymer additives, and it is unclear whether the parameter providing the best correlation is molecular weight, chain length, radius of gyration, hydrodynamic volume, or a combination of these.

Virk [67] correlated the onset of DR with radius of gyration, which depends on both polymer molecular weight and polymer/solvent interactions. DR efficiency varies with polymer concentration, molecular weight, and chain length, whereas the coil dimension is considered to be as important as molecular weight [68,69]. McCormick *et al.* [69] suggested that good DR can be achieved by low-molecular-weight polymers if their concentrations are high enough (Figure 14). However, they pointed out that there might be a low-molecular-weight limit for effective DR.

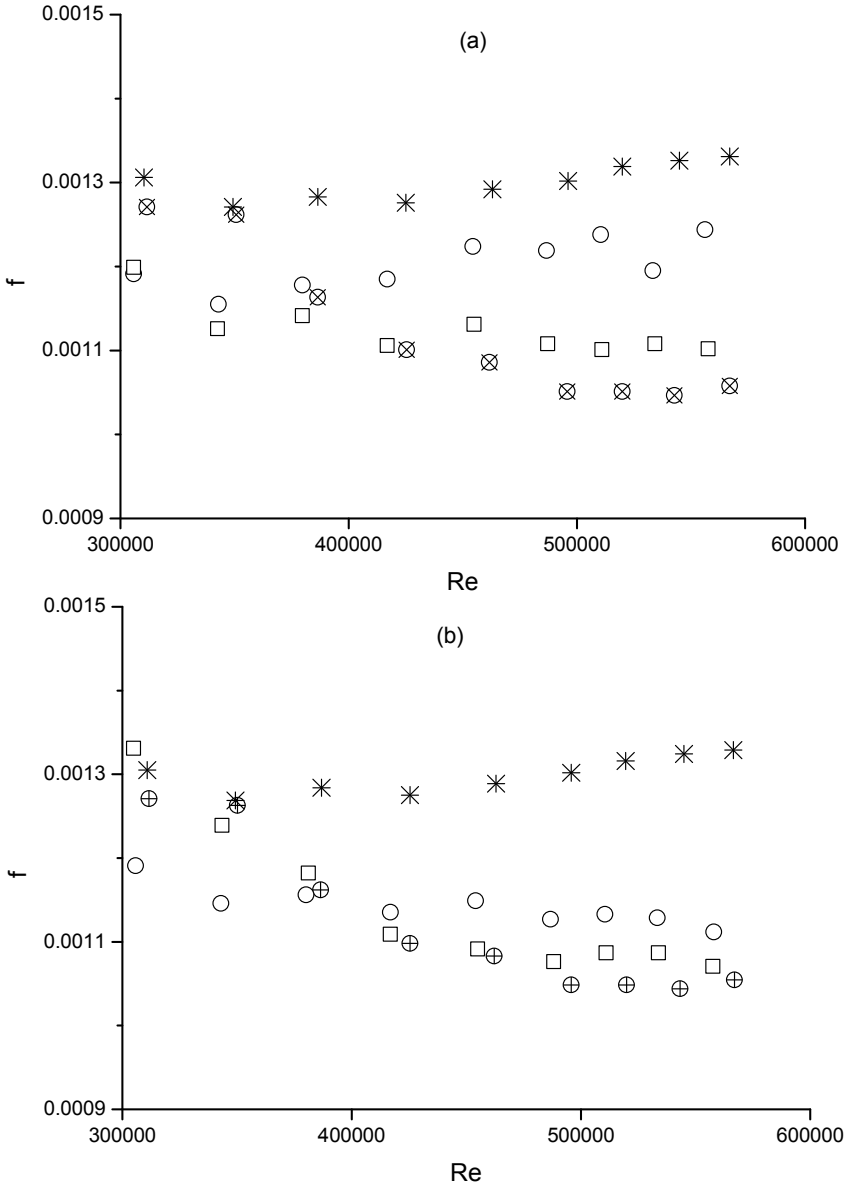

Figure 14. *Cont.*

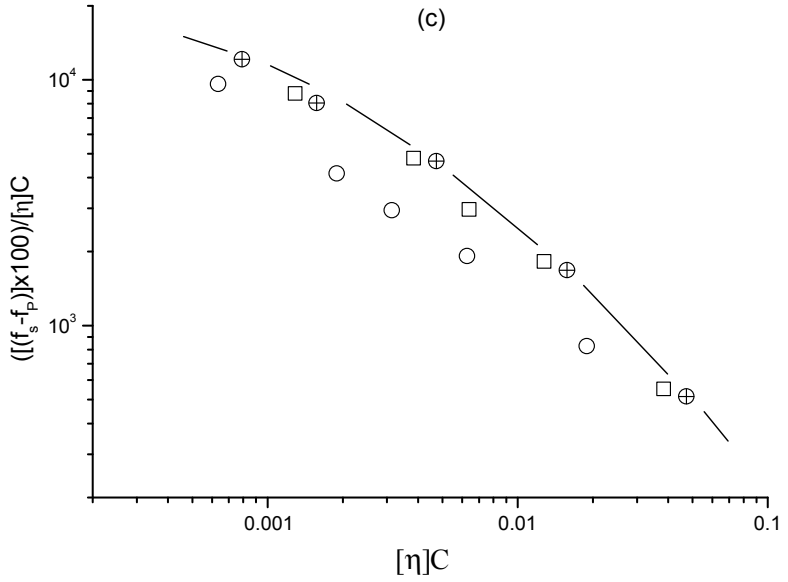

Figure 14. Drag reduction behavior of PEO polymers in 0.514 M NaCl tested by rotating disk: solvent (*); WSR-N-12K, M_W = 1.7 × 10^6 (○), WSR-N-60K, M_W = 4.0 × 10^6 (□); WSR-301, M_W = 5.3 × 10^6 (□). (**a**) Friction factor *versus* Reynolds number for 3 ppm PEO solutions; (**b**) Friction factor *versus* Reynolds number at constant polymer volume fraction, $[\eta]C$ = 0.007; (**c**) Drag reduction efficiency measured at *R*e = 520,000 *versus* PEO polymer volume fraction (Reprinted from [68]).

Furthermore, Gampert and Wagner [70] suggested that DR efficiency might be correlated using the Deborah number, N_{De}, which depends on polymer molecular weight and relaxation time as follows [71]:

$$N_{De} = \frac{([\eta]\eta_s MW)/(N_A kT)}{\tau_w/\eta} \quad (5)$$

where [η] is the intrinsic viscosity, *M* is molecular weight, *k* is the Boltzmann constant, *T* is absolute temperature, and N_A is Avogadro's number. A single curve for polymers with different molecular weights was obtained when DR (reduced for polymer volume fraction DR(%) $[\eta]C$) was plotted against N_{De}. Here, *C* is the polymer concentration.

In addition, the enhancement of DR by high-molecular-weight molecules with a polydispersed sample was shown [72,73] for hydrocarbon-soluble polymers. Their data suggested that a minimum molecular weight, which is unique for each polymer system, is required before a polymer can effectively reduce drag. They also demonstrated the importance of coil volume, rather than polymer molecular weight, by studying a number of hydrocarbon-soluble polymers in various solvents. Recently, by studying the DR of oil-soluble polyisobutylene (PIB) in different organic solvents, Choi *et al.* [74] observed that better DR occurred in good solvents. Therefore, for a fixed polymer molecular weight and concentration, DR efficiency will be enhanced in solvents with larger values of [η]. For a given polymer in various solvents, equal DR efficiency was demonstrated at equal values of the polymer volume fraction, $[\eta]C$ [69]. That is, at constant polymer molecular weight and concentration, DR effectiveness increases in the solvent in which the polymer chain volume increases.

In addition, mechanical shear degradation of the polymer chains makes it difficult to understand the effect of molecular weight on DR. In many DR experiments, molecular weight and molecular weight

distribution change due to shear degradation. Molecular weight distribution experiments have demonstrated that the higher its fraction, which is responsible for a larger amount of DR, the more susceptible it is to shear degradation, and thus the DR performance will be adversely affected.

7. Reynolds Number Effect

Turbulent flow is produced for sufficiently high Reynolds numbers, $Re = \rho D u_{av}/\eta$, where D is the diameter of a pipe or disk, u_{av} is the average flow velocity, ρ is the fluid mass density, and η is the fluid viscosity. Meanwhile, the formation of what is known as the maximum DR asymptote has been revealed. Usually, maximum DR can be achieved in a dilute polymer solution by even minute amounts of suitable polymers [75]. As a maximum DR asymptote, the power-law form equation was reported from correlating the DR and the Reynolds number.

At different ranges of Reynolds number, different DR efficiencies were observed [76]. As the Reynolds number increased, the efficiency of a polymer additive in decreasing the hydraulic resistance of the flow increased, but only up to a certain value of the Reynolds number. When $Re \leq 2.3 \times 10^3$ for a laminar flow of polymer solutions in a pipe flow, the magnitude of the DR effect is either zero or negative, *i.e.*, polymer additives lead to an increase in the effective viscosity and, naturally, do not act as agents to reduce the resistance to the flow. No DR was observed at Reynolds numbers below 3×10^5 using a rotating disk flow system [77]. When $Re > (3–5) \times 10^3$, the DR effect comes into play and, as the Re increases, the magnitude of the DR effect increases until reaching a maximum.

Obviously, different Reynolds numbers can control the flow structure, as shown in Figure 15 with the conceptual model [40]. These conceptual models can help us to understand the DR of polymer solutions at different Reynolds numbers. Furthermore, it can be also noted that for a riblet-lined pipe, different DR efficiency was demonstrated compared to a smooth pipe [78].

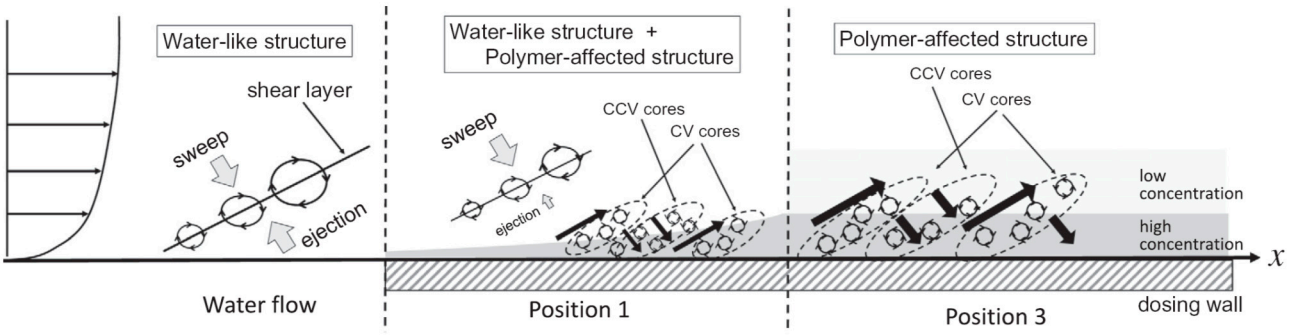

Figure 15. Conceptual model for the streamwise variation of the turbulent structure (Reprinted from [40]).

8. Temperature Effect

Operating temperature is an important parameter in DR, especially in terms of engineering applications. Interthal and Wilski [79] studied the effects of temperature on the DR with both PEO and partially hydrolyzed PAAM of 30 ppm each in a pipe turbulent flow. They showed that the DR of 80% achieved for PAAM was not affected by the temperature, which was increased from 5 to 35 °C, but the

DR of PEO changed from 70% to 50% in the same temperature range. This decrease was considered to be due to a reduction in solvation of the polymer molecules as the temperature increased.

As shown in Figure 16, another study on the effect of temperature on DR was further examined with 50 wppm PAAM and PEO at three different temperatures [54]. For PAAM, the temperature elevation resulted in an increase in the initial DR without noticeable degradation. With PEO, on the other hand, the advantage of a larger initial DR with higher temperature was lost due to an increased rate in degradation. However, whether these temperature effects would be the same for all polymers or not needs further investigation.

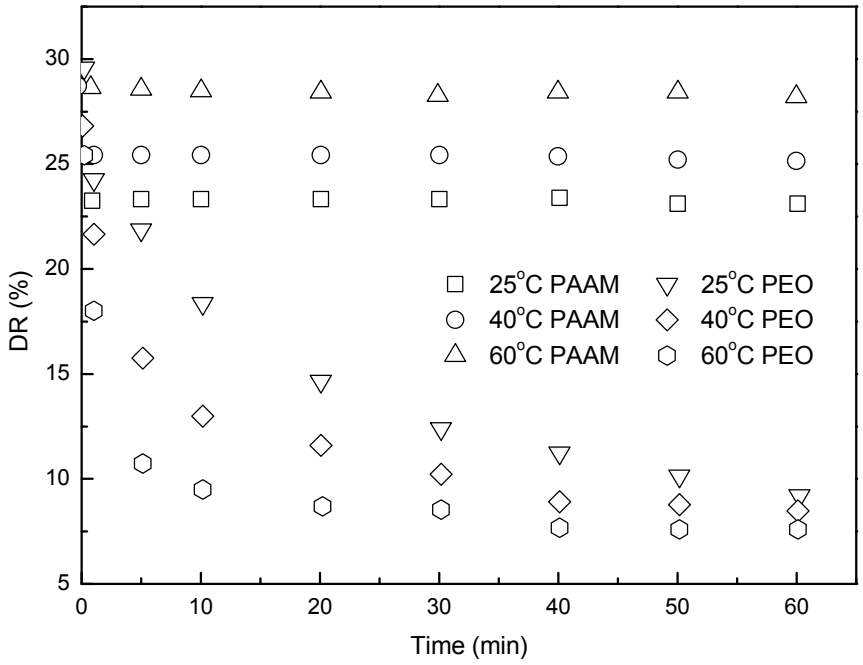

Figure 16. Drag reduction of 50 wppm PAAM and PEO at three different temperatures (Reprinted from [80]).

In addition, turbulent DR of the water-soluble PEO when it approaches its theta temperature was examined [80]. The results clearly demonstrated that the DR properties of the polymer additive were sensitive to the distance away from their theta temperatures, even at very low polymer concentrations.

9. Conclusion

In this feature article, polymer additives and experimental factors affecting turbulent DR are briefly reviewed for rotating disk flow in addition to pipe flow. The flexibility and concentration of the polymers applied, in addition to polymer molecular weight and polymer/solvent interactions, determine the level of DR. Polymer conformation is regarded to be one of the most important factors affecting DR efficiency. Therefore, to control flow structure or polymer chain conformation in turbulent flow, Reynolds number, temperature, and flow geometry need to be carefully controlled.

Acknowledgments

This work was supported by National Research Foundation of Korea (2010).

References

1. Ranade, V.V.; Mashelkar, R.A. Turbulent mixing in dilute polymer-solutions. *Chem. Eng. Sci.* **1993**; *48*, 1619–1628.
2. Abdulbari, H.A.; Shabirin, A.; Abdurrahman, H.N. Bio-polymers for improving liquid flow in pipelines—A review and future work opportunities. *J. Ind. Eng. Chem.* **2014**, *20*, 1157–1170.
3. Abubakar, A.; Al-Wahaibi, T.; Al-Wahaibi, Y.; Al-Hashmi, A.R.; Al-Ajmi, A. Roles of drag reducing polymers in single- and multi-phase flows. *Chem. Eng. Res. Des.* **2014**, *92*, 2153–2181.
4. Ilg, P.; de Angelis, E.; Karlin, I.V.; Casciola, C.M.; Succi, S. Polymer dynamics in wall turbulent flow. *Europhys. Lett.* **2002**, *58*, 616–622.
5. Manzhai, V.N.; Nasibullina, Y.R.; Kuchevskaya, A.S.; Filimoshkin, A.G. Physico-chemical concept of drag reduction nature in dilute polymer solutions (the Toms effect). *Chem. Eng. Process.* **2014**, *80*, 38–42.
6. Dosunmu, I.T.; Shah, S.N. Turbulent flow behavior of surfactant solutions in straight pipes. *J. Petrolem Sci. Eng.* **2014**, *124*, 323–330.
7. Yang, J.W.; Park, H.; Chun, H.H.; Ceccio, S.L.; Perlin, M.; Lee, I. Development and performance at high Reynolds number of a skin-friction reducing marine paint using polymer additives. *Ocean Eng.* **2014**, *84*, 183–193.
8. Fu, Z.; Otsuki, T.; Motozawa, M.; Kurosawa, T.; Yu, B.; Kawaguchi, Y. Experimental investigation of polymer diffusion in the drag-reduced turbulent channel flow of inhomogeneous solution. *Int. J. Heat. Mass. Trans.* **2014**, *77*, 860–873.
9. Tamano, S.; Kitao, T.; Morinishi, Y. Turbulent drag reduction of boundary layer flow with non-ionic surfactant injection. *J. Fluid Mech.* **2014**, *749*, 367–403.
10. Tamano, S.; Ikarashi, H.; Morinishi, Y.; Taga, K. Drag reduction and degradation of nonionic surfactant solutions with organic acid in turbulent pipe flow. *J. Non-Newton. Fluid Mech.* **2015**, *215*, 1–7.
11. Suzuki, H.; Shingo, T.; Komoda, Y. Direct numerical simulation of the turbulent channel flow of a polymer solution. *Int. J. Refrig.* **2010**, *33*, 1632–1638.
12. Steele, A.; Bayer, I.S.; Loth, E. Pipe flow drag reduction effects from carbon nanotube additives. *Carbon* **2014**, *77*, 1183–1186.
13. Boffetta, G.; Mazzino, A.; Musacchio, S.; Vozella, L. Polymer heat transport enhancement in thermal convection: The case of Rayleigh-Taylor turbulence. *Phys. Rev. Lett.* **2010**, *104*, 184501.
14. Burger, E.D.; Chorn, L.G. Studies of drag reduction conducted over a broad range of pipeline conditions when flowing prudhoe bay crude oil. *J. Rheol.* **1980**, *24*, 603–626.
15. Usui, H.; Li, L.; Suzuki, H. Rheology and pipeline transportation of dense fly ash-water slurry. *Korea-Aust. Rheol. J.* **2001**, *13*, 47–54.
16. Greene, H.L.; Mostardi, R.F.; Nokes, R.F. Effects of drag reducing polymers on initiation of atherosclerosis. *Polym. Eng. Sci.* **1980**, *20*, 499–504.

17. Marhefka, J.N.; Marascalco, P.J.; Chapman, T.M.; Russell, A.J.; Kameneva, M.V. Poly(*N*-vinylformamide)—A drag-reducing polymer for biomedical applications. *Biomacromolecules* **2006**, *7*, 1597–1603.
18. Fontaine, A.A.; Deutsch, S.; Brungart, T.A.; Petrie, H.L.; Fenstermacker, M. Drag reduction by coupled systems: Microbubble injection with homogeneous polymer and surfactant solutions. *Exp. Fluids* **1999**, *26*, 397–403.
19. Lumley, J.L. Drag reduction in turbulent flow by polymer additives. *J. Polym. Sci.* **1973**, *7*, 263–290.
20. Astarita, G. Possible interpretation of mechanism of drag reduction in viscoelastic liquids. *Ind. Eng. Chem. Fundam.* **1965**, *4*, 354–356.
21. Gadd, G.E. Turbulence damping and drag reduction produced by certain additives in water. *Nature* **1965**, *206*, 463–467.
22. Walsh, M. Theory of drag reduction in dilute high-polymer flows. *Int. Shipbuilding Prog.* **1967**, *14*, 134.
23. Gadd, G.E. Reduction of turbulent drag in liquids. *Nat. Phys. Sci.* **1971**, *230*, 29–31.
24. Kuo, Y.; Tanner, R.I. A burgers-type model of turbulent decay in a non-newtonian fluid. *J. Appl. Mech.* **1972**, *39*, 661–666.
25. Gordon, R.J.; Balakrishnan, C. Vortex inhibition: A new viscoelastic effect with importance in drag reduction and polymer characterization. *J. Appl. Polym. Sci.* **1972**, *16*, 1629–1639.
26. Armstrong, R.; Jhon, M.S. Turbulence induced change in the conformation of polymer molecules. *J. Chem. Phys.* **1983**, *79*, 3143–3147.
27. Fraenkel, G.K. Visco-elastic effect in solutions of simple particles. *J. Chem. Phys.* **1952**, *20*, 642–647.
28. Brostow, W. Drag reduction and mechanical degradation in polymer solutions in flow. *Polymer* **1983**, *24*, 631–638.
29. Brostow, W.; Majumdar, S.; Singh, R.P. Drag reduction and solvation in polymer solutions. *Macromol. Rapid. Commun.* **1999**, *20*, 144–147.
30. Tabor, M.; de Gennes, P.G. A cascade theory of drag reduction. *Europhys. Lett.* **1986**, *2*, 519–522.
31. Valente, P.C.; da Silva, C.B.; Pinho, F.T. The effect of viscoelasticity on the turbulent kinetic energy cascade. *J. Fluid Mech.* **2014**, *760*, 39–62.
32. Jourdan, L.; Knapp, Y.; Oliver, F.; Guibergia, J.P. The effect of drag-reducing polymer additives on wall-pressure fluctuations in turbulent channel flows. *Eur. J. Mech. B-Fluid.* **1998**, *17*, 105–136.
33. Gillissen, J.J.J.; Boersma, B.J.; Mortensen, P.H.; Andersson, H.I. Fibre-induced drag reduction. *J. Fluid Mech.* **2008**, *602*, 209–218.
34. Paschkewitz, J.S.; Dimitropoulos, C.D.; Hou, Y.X.; Somandepalli, V.S.R.; Mungal, M.G.; Shaqfeh, E.S.G.; Moin, P. An experimental and numerical investigation of drag reduction in a turbulent boundary layer using a rigid rodlike polymer. *Phys. Fluids* **2005**, *17*, doi:10.1063/1.1993307.
35. Choi, H.J.; Lim, S.T.; Lai, P.Y.; Chan, C.K. Turbulent drag reduction and degradation of DNA. *Phys. Rev. Lett.* **2002**, *89*, 088302.
36. Brostow, W. Drag reduction in flow: Review of applications, mechanism and prediction. *J. Ind. Eng. Chem.* **2008**, *14*, 409–416.

37. Pereira, A.S.; Soares, E.J. Polymer degradation of dilute solutions in turbulent drag reducing flows in a cylindrical double gap rheometer device. *J. Non-Newton. Fluid Mech.* **2012**, *179*, 9–22.
38. Chemloul, N.S. Experimental study of the drag reduction in turbulent pipe flow. *Energy* **2014**, *64*, 818–827.
39. Karami, H.R.; Mowla, D. A general model for predicting drag reduction in crude oil pipelines. *J. Petrol. Sci. Eng.* **2013**, *111*, 78–86.
40. Motozawa, M.; Sawada, T.; Ishitsuka, S.; Iwamoto, K.; Ando, H.; Senda, T.; Kawaguchi, Y. Experimental investigation on streamwise development of turbulent structure of drag-reducing channel flow with dosed polymer solution from channel wall. *Int. J. Heat Fluid Flow* **2014**, *50*, 51–62.
41. Moussa, T.; Tiu, C.; Sridhar, T. Effect of solvent on polymer degradation in turbulent-flow. *J. Non-Newton. Fluid Mech.* **1993**, *48*, 261–284.
42. Kim, C.A.; Jo, D.S.; Choi, H.J.; Kim, C.B.; Jhon, M.S. A high-precision rotating disk apparatus for drag reduction characterization. *Polym. Test.* **2001**, *20*, 43–48.
43. Ricco, P.; Hahn, S. Turbulent drag reduction through rotating discs. *J. Fluid Mech.* **2013**, *722*, 267–290.
44. Wise, D.J.; Alvarenga, C.; Ricco, P. Spinning out of control: Wall turbulence over rotating discs. *Phys. Fluids* **2014**, *26*, doi:10.1063/1.4903973.
45. Wise, D.J.; Ricco, P. Turbulent drag reduction through oscillating discs. *J. Fluid Mech.* **2014**, *746*, 536–564.
46. Sreedhar, I.; Jain, G.; Srinivas, P.; Reddy, K.S.K. Polymer induced turbulent drag reduction using pressure and gravity-driven methods. *Korean J. Chem. Eng.* **2014**, *31*, 568–573.
47. Burnishev, Y.; Steinberg, V. Early turbulence in von Karman swirling flow of polymer solutions. *Europhys. Lett.* **2015**, *109*, doi:10.1209/0295-5075/109/14006.
48. Eskin, D. Applicability of a Taylor-Couette device to characterization of turbulent drag reduction in a pipeline. *Chem. Eng. Sci.* **2014**, *116*, 275–283.
49. Moosaie, A.; Manhart, M. Direct Monte Carlo simulation of turbulent drag reduction by rigid fibers in a channel flow. *Acta Mech.* **2013**, *224*, 2385–2413.
50. Wang, S.N.; Graham, M.D.; Hahn, F.J.; Xi, L. Time-series and extended Karhunen-Loeve analysis of turbulent drag reduction in polymer solutions. *AIChE J.* **2014**, *60*, 1460–1475.
51. Amrouchene, Y.; Kellay, H. Polymer in 2D turbulence: Suppression of large scale fluctuation. *Phys. Rev. Lett.* **2002**; *89*, doi:10.1103/PhysRevLett.89.104502.
52. Hidema, R.; Suzuki, H.; Hisamatsu, S.; Komoda, Y. Characteristic scales of two-dimensional turbulence in polymer solutions. *AIChE J.* **2014**, *60*, 1854–1862.
53. Jun, Y.; Zhang, J.; Wu, X.L. Polymer effect on small and large scale two-dimensional turbulece. *Phys. Rev. Lett.* **2006**, *96*, doi:10.1103/PhysRevLett.96.024502.
54. Sung, J.H.; Kim, C.A.; Choi, H.J.; Hur, B.K.; Kim, J.G.; Jhon, M.S. Turbulent drag reduction efficiency and mechanical degradation of poly(acrylamide). *J. Macromol. Sci. Phys.* **2004**, *B43*, 507–518.
55. Zhang, K.; Choi, H.J.; Jang, C.H. Turbulent drag reduction characteristics of poly(acrylamide-*co*-acrylic acid) in a rotating disk apparatus. *Colloid Polym. Sci.* **2011**, *289*, 1821–1827.

56. Brostow, W.; Drewniak, M. Computer simulations of chain conformations in dilute polymer solutions under shear flow. *J. Chem. Phys.* **1996**, *105*, 7135–7139.
57. Ram, P.S.; Pal, S.; Krishnamoorthy, S.; Adhikary, P.; Ali, A.S. High-technology materials based on modified polysaccharides. *Pure Appl. Chem.* **2009**, *81*, 525–547.
58. Halake, K.; Birajdar, M.; Kim, B.S.; Bae, H.; Lee, C.C.; Kim, Y.J.; Kim, S.; Kim, H.J.; Ahn, S.; An, Y.; *et al*. Recent application developments of water-soluble synthetic polymers. *J. Ind. Eng. Chem.* **2014**, *20*, 3913–3918.
59. Kim, C.A.; Choi, H.J.; Kim, C.B.; Jhon, M.S. Drag reduction characteristics of polysaccharide xanthan gum. *Macromol. Rapid Commun.* **1998**, *19*, 419–422.
60. Lim, S.T.; Choi, H.J.; Biswal, D.; Singh, R.P. Turbulent drag reduction characteristics of amylopectin and its derivative. *E-Polymers* **2004**, *4*, doi.10.1515/epoly.2004.4.1.751.
61. Lim, S.T.; Choi, H.J.; Lee, S.Y.; So, J.S.; Chan, C.K. Gamma-DNA induced turbulent drag reduction and its characteristics. *Macromolecules* **2003**, *36*, 5348–5354.
62. Hong, C.H.; Zhang, K.; Choi, H.J.; Yoon, S.M. Mechanical degradation of polysaccharide guar gum under turbulent flow. *J. Ind. Eng. Chem.* **2010**, *16*, 178–180.
63. White, C.M.; Somandepalli, V.S.R.; Mungal, M.G. The turbulence structure of drag-reduced boundary layer flow. *Exp. Fluids* **2004**, *36*, 62–69.
64. Kim, C.A.; Choi, H.J.; Sung, J.H.; Lee, H.M.; Jhon, M.S. Effect of solubility parameter of polymer-solvent pair on turbulent drag reduction. *Macromol. Symp.* **2005**, *222*, 169–174.
65. Sohn, J.I.; Kim, C.A.; Choi, H.J.; Jhon, M.S. Drag-reduction effectiveness of xanthan gum in a rotating disk apparatus. *Carbohyd. Polym.* **2001**, *45*, 61–68.
66. Lim, S.T.; Choi, H.J.; Chan, C.K. Effect of turbulent flow on coil-globule transition of lambda-DNA. *Macromol. Rapid. Commun.* **2005**, *26*, 1237–1240.
67. Virk, P.S. Drag reduction fundamentals. *AIChE J.* **1975**, *21*, 625–656.
68. McCormick, C.L.; Hester, R.D.; Morgan, S.E.; Safieddine, A.M. Water-soluble copolymers .31. Effects of molecular-parameters, solvation, and polymer associations on drag reduction performance. *Macromolecules* **1990**, *23*, 2132–2139.
69. McCormick, C.L.; Hester, R.D.; Morgan, S.E.; Safieddine, A.M. Water-soluble copolymers .30. Effects of molecular structure on drag reduction efficiency. *Macromolecules* **1990**, *23*, 2124–2131.
70. Gampert, B.; Wagner, P. *The Influence of Polymer Additives on Velocity and Temperature Fields*; Springer-Verlag: Berlin, Germany, 1985.
71. Morgan, S.E.; McCormick, C.L. Water-Soluble copolymers XXXII: Macromolecular drag reduction. A review of predictive theories and the effects of polymer structure. *Prog. Polym. Sci.* **1990**, *15*, 507–549.
72. Liaw, G.C.; Zakin, J.L.; Patterson, G.K. Effect of molecular parameters, solvation, and polymer associations on drag reductioin. *AIChE J.* **1971**, *17*, 391–397.
73. Zakin, J.L.; Hunston, D.L. Effect of polymer molecular variables on drag reduction. *J. Macromol. Sci. Phys.* **1980**, *18*, 795–814.
74. Choi, H.J.; Kim, C.A.; Jhon, M.S. Universal drag reduction characteristics of polyisobutylene in a rotating disk apparatus. *Polymer* **1999**, *40*, 4527–4530.
75. Virk, P.S.; Merrill, E.W.; Mickley, H.S.; Smith, K.A.; Mollo-Christensen, E.L. The Toms phenomenon: Turbulent pipe flow polymer solutions. *J. Fluid Mech.* **1967**, *20*, 305–328.

76. Myagchenkov, V.A.; Chichkanov, S.V. Toms effect in model and real systems. *Russ. J. Appl. Chem.* **2005**, *78*, 521–537.
77. Choi, H.J.; Jhon, M.S. Polymer-induced turbulent drag reduction. *Ind. Eng. Chem. Res.* **1996**, *35*, 2993–2998.
78. Koury, E.; Virk, P.S. Drag reduction by polymer solutions in a riblet-lined pipe. *Appl. Sci. Res.* **1995**, *54*, 323–347.
79. Interthal, W.; Wilski, H. Drag reduction experiments with very large pipes. *Colloid Polym. Sci.* **1985**, *263*, 217–229.
80. Lim, S.T.; Hong, C.H.; Choi, H.J.; Lai, P.-Y.; Chan, C.K. Polymer turbulent drag reduction near the theta point. *Europhys. Lett.* **2007**, *80*, 58003.